Available online at www.sciencedirect.com
SCIENCE DIRECT®
International Journal of Heat and Mass Transfer 48 (2005) 1926–1935
International Journal of HEAT and MASS TRANSFER
www.elsevier.com/locate/ijhmt

An experimental study on local interfacial area concentration using a double-sensor probe

Zhao Dongjian, Guo Liejin *, Lin Changzhi, Zhang Ximin

State Key Laboratory of Multiphase Flow in Power Engineering, Xi'an Jiaotong University, Xi'an 710049, China

Received 18 May 2004; received in revised form 1 December 2004
Available online 4 March 2005

Abstract

Interfacial area concentration is an important parameter in modeling the interfacial transfer terms in the two-fluid model. In this paper, the interfacial area concentration, void fraction, and bubble Sauter mean diameter for air–water bubbly flow through a vertical transparent pipe with 40 mm internal diameter was investigated experimentally using both digital high-speed camera system and a double-sensor conductivity probe. Based on the experimental data of digital high-speed camera system, the statistical models derived by different researchers for local interfacial area concentration measurement using double-sensor conductivity probe were evaluated. The results show that there are obvious differences among the values of local interfacial area concentration calculated by different statistical models even from the same probe signals. The section-averaged values of the local interfacial area concentration calculated using the statistical model by Kataoka et al. agree best with experimental data of digital high-speed camera system. Therefore, the statistical model developed by Kataoka et al. is recommended for the local measurement of interfacial area concentration using a double-sensor conductivity probe in bubbly two-phase flow. Using the verified double-sensor probe method, we carry out experiment to study the local distribution characteristic of the interfacial area concentration and void fraction in air–water bubbly flow through a vertical pipe.

Keywords: Interfacial area concentration; Double-sensor conductivity probe; Digital high-speed camera system; Void fraction; Bubble Sauter mean diameter

1. Introduction

Because of the complicated transfer mechanisms at the interface coupled with the motion and distortion of the interface, the constitutive equations for interfacial transfer terms are the weakest link in two-fluid model. Interfacial area concentration represents the effective area in which mass, momentum or energy transfer occurs between phases [1]. According to Ishii [2], the interfacial transfer terms could be expressed in terms of interfacial area concentration and the driving force. In view of the importance of interfacial area concentration, many researchers [3–11] have carried out experimental works to study the distribution of interfacial area concentration in turbulent bubbly flow. Local experimental data of interfacial area concentration have been published for gas–liquid flows in vertical round pipes [3–5]. Additional two-phase flow interfacial area concentration measurements have been carried out in horizontal

* Corresponding author. Tel.: +86 29 82668769/3895; fax: +86 29 82668769/9033.
E-mail address: lj-guo@mail.xjtu.edu.cn (L. Guo).

0017-9310/$ - see front matter © 2005 Elsevier Ltd. All rights reserved.
doi:10.1016/j.ijheatmasstransfer.2004.12.009

Nomenclature

a	minor axis length of ellipsoidal bubble (m)
a_i	time-averaged interfacial area concentration (m^{-1})
A	interfacial area of a bubble (m^2)
b	major axis length of ellipsoidal bubble (m)
d_{sm}	bubble Sauter mean diameter (m)
$f(V)$	bubble size probability distribution function (m^{-3})
N_b	bubbles number of sampling (dimensionless)
N_{miss}	missed bubbles number of sampling (dimensionless)
N_t	bubbles number of passing the probe per unit time (s^{-1})
Δs	distance between two tips of the probe (m)
ΔT	sampling time (s)
$V'_b/\overline{V}_b$	relative bubble velocity fluctuation (dimensionless)
V_j	volume of the group-j bubbles (m^3)
$\vec{v}_{sz}$	z component of the interfacial velocity (m/s)

Greek symbols

α	time-averaged void fraction (dimensionless)
α_0	maximum angle between the interfacial velocity and the mean flow direction (dimensionless)
σ_z	root mean square of z component of the velocity fluctuations (m/s)

Subscripts

DF	falling signal of downstream sensor
DR	rising signal of downstream sensor
UF	falling signal of upstream sensor
UR	rising signal of upstream sensor

pipes [6–8], subcooled boiling flow [12], an annulus [9], and confined channels [10,11]. Various measuring techniques have been developed, which include local probes [3–5,13–16] (e.g., conductivity probes, fiber–optic probes), photography [12,17], ultrasonic attenuation [18], and chemical method [19–21]. The double-sensor conductivity probe method, with the capability to measure the local interfacial area concentration, becomes one of most widely used measurement techniques for obtaining local parameters in two-phase bubbly flow. It consists of two sensors that detect gas and liquid phases from the difference of their electrical resistivities. In order to use this method, it is most important to establish the statistical model that relates the local interfacial area concentration to some easily measurable quantities.

Over the past twenty years, different statistical models for local interfacial area concentration measurement using a double-sensor probe have been developed. According to Kataoka et al. [14], Sekoguchi et al. [15] used firstly this technique for local interfacial area concentration measurement in 1974, and the interfacial area concentration was estimated by the number of bubbles passing the probe per unit time and the measured velocity of the bubble. The authors assumed that the bubble velocity is constant and have a component of main flow direction only. In the actual turbulent bubbly flow, however, bubbles have various velocity components other than the main flow direction. Considering firstly this effect, Kataoka et al. [3] proposed a widely used statistical model for local interfacial area concentration measurement in bubbly flow using double-sensor probe method. Recently, Hibiki et al. [5] improved the probability density function of the angle between the bubble interfacial velocity and the main flow direction, and developed further this model. Wu and Ishii [13] considered the missed bubble contribution to the interfacial area concentration is higher than a normal bubble, because the missed bubble are smaller bubble or the bubbles caught on the edge. Based on the measurement of bubble size probability distribution function from double-sensor probe signal, Kalkach-Navarro et al. [4] also derived such a statistical model. At the present time, however, no work has been carried out on comparison and evaluation of the accuracy and reliability of different statistical models.

Dias et al. [16] also suggested a statistical method for local interfacial area concentration measurement from the bubble actual velocity. They assumed the angle between the bubble interfacial velocity and the main flow direction was uniformly distributed within a solid angle (the same assumption as Kataoka et al. [3]). But they used another probability density function of that angle on the derivation of their model. Kiambi et al. [22] used the relation suggested by Kataoka et al. [3] for local interfacial area concentration calculation. But for the unknown maximum angle between the bubble interfacial velocity and the main flow direction, they used a expression proposed by Dias et al. [16]. However, the two equations is derived based on different assumption on the distributions of the angle between the bubble interfacial velocity and the main flow direction, and the angle between the interfacial velocity and the normal vector of the interface.

In this paper, the local interfacial area concentration for air–water bubbly flow through a vertical pipe was investigated experimentally using both digital

high-speed camera system and a double-sensor conductivity probe. Based on the experimental data of digital high-speed camera system, the different statistical models for local interfacial area concentration measurement using double-sensor conductivity probe were compared and evaluated.

2. Several statistical models for local interfacial area concentration measurement

2.1. Kataoka's statistical model [3]

According to the definition of the local interfacial area concentration by Ishii [2], Kataoka et al. [3] carried out derivations and established a statistical model that related the local time-averaged interfacial area concentration to the harmonic mean of the interfacial velocity. Here we consider the main flow is in the Z direction. Assuming that the bubbles were spherical, the probe passed every part of the bubbles with an equal probability, and there was no statistical relation between interfacial velocity and the angle between the interfacial velocity and the normal vector of the interface, this statistical model can be expressed as

$$\bar{a}_i^t = 4N_t\left(\overline{\frac{1}{|\vec{v}_{szj}|}}\right)\cdot\frac{1}{1-\cot\frac{\alpha_0}{2}\ln\left(\cos\frac{\alpha_0}{2}\right)-\tan\frac{\alpha_0}{2}\ln\left(\sin\frac{\alpha_0}{2}\right)}, \tag{1}$$

where $\vec{v}_{szj}$, α_0 and N_t denote z component of the interfacial velocity, the maximum angle between the interfacial velocity and the mean flow direction, and the number of bubbles measured per unit time, respectively. On the derivation of Eq. (1), it was also assumed that the angle between the bubble interfacial velocity and the main flow direction, α, was random with an equal probability within some maximum angle α_0. The value of α_0 was determined from the statistical parameters of the measured interfacial velocity. Assuming that the interfacial velocity fluctuations in three directions were equilateral, Kataoka et al. [3] derived the relationship between the maximum angle α_0 and the standard deviation of bubble velocity fluctuation in the main flow direction with the following form

$$\frac{\sin 2\alpha_0}{2\alpha_0} = \frac{1-\sigma_z^2/\overline{|\vec{v}_{szj}|}^2}{1+3\sigma_z^2/\overline{|\vec{v}_{szj}|}^2}, \tag{2}$$

where σ_z denotes the root mean square of the interface velocity fluctuation. For more details on the mathematical modeling of this measurement method, one can refer to [3].

2.2. Kalkach-Navarro's statistical model [4]

Kalkach-Navarro et al. [4] assumed that the bubbles were spherical and the bubble sizes were represented by a probability distribution function, $f(V_j)$, where $f(V_j)\Delta V$ was the number of bubbles per unit volume having a volume between V_j and $V_j+\Delta V$. From the geometrical consideration, Kalkach-Navarro et al. [4] proposed the following statistical model for local interfacial area concentration measurement

$$\bar{a}_i^t = (36\pi)^{1/3}\sum_j f(V_j)V_j^{2/3}\Delta V_j, \tag{3}$$

where V_j was the volume of the group-j bubbles and calculated from the chord length measured by a double-sensor probe. In order to determine $f(V_j)$, the maximum chord length measured was divide into equal partitions, then a probability of each partition of chord length was obtained. Assuming the bubbles could be penetrated at any point with equal probability by the sensors, a triangular matrix, which represented the relationship between the probability of the chord length cut by sensors and the probability of bubble radius, was established. Then, the bubble size probability distribution function, $f(V_j)$, could be derived from the probability distribution of the bubble radius. In this model, however, the authors derived straightway the relations for local IAC measurement from the chord length distributions, and took no account for the effect of bubble lateral motions.

2.3. Hibiki's statistical model [5]

As reported by Hibiki et al. [5], Wu et al. recently conducted a similar derivation to Kataoka et al. [3] based on basically the same assumptions, except for the probability density function of α, the angle between the bubble interfacial velocity and the main flow direction. In view that the probability density function of α had a peak in the main flow direction from the experimental data, Wu et al. [5] replaced the equal probability within a maximum angle of, α, using the following relations:

$$g(\alpha) = \begin{cases} \frac{1}{\alpha_0^3}(\alpha-\alpha_0)^2 & \text{for } 0\leqslant\alpha\leqslant\alpha_0, \\ 0 & \text{for } \alpha_0\leqslant\alpha\leqslant\pi/2. \end{cases} \tag{4}$$

The final statistical relation for local time-averaged interfacial area concentration measurement is written as

$$\bar{a}_i^t = 2N_t\left(\overline{\frac{1}{|\vec{v}_{szj}|}}\right)\cdot\frac{\alpha_0^3}{3(\alpha_0-\sin\alpha_0)}. \tag{5}$$

Based on the similar considerations as Kataoka et al. [3], Wu et al. [5] derived the following relations between the maximum angle, α_0, and the standard deviation of bubble velocity fluctuation in the main flow direction

$$\frac{3}{2\alpha_0^2}\left(1-\frac{\sin 2\alpha_0}{2\alpha_0}\right) = \frac{1-\sigma_z^2/\overline{|\vec{v}_{sz}|}^2}{1+3\sigma_z^2/\overline{|\vec{v}_{sz}|}^2}. \tag{6}$$

2.4. Wu's statistical model [13]

Wu and Ishii [13] carried out sensitivity study through numerical method on double-sensor conductivity probe measuring local interfacial area concentration. They assumed that the bubble velocity fluctuation was isotropic and the bubble was spherical. Considering the effects of bubble lateral motions and the distance between the two tips of the double-sensor probe, and taking the contribution of the missed bubbles into account, a statistical model was obtained also from the definition by Ishii [2] as

$$\bar{a}_i^t = \frac{2N_b}{\Delta T(N_b - N_{miss})} \cdot \left[2 + \left(\frac{V'_b}{\overline{V}_b}\right)^{2.25}\right] \left(\overline{\frac{1}{\vec{v}_{szj}}}\right), \tag{7}$$

where $\Delta T, N_b, N_{miss}$, and $V'_b/\overline{V}_b$ denotes the sampling time, the total number of measured bubbles, the number of the missed bubbles, and relative bubble velocity fluctuation, respectively. The missed bubbles referred to those that were touched by the first sensor but not by the second sensor, or those that passed the second sensor ahead of the first sensor in view of the bubble lateral motions. The number of the missed bubbles could be obtained from the double-sensor probe signals directly. From numerical method, Wu and Ishii [13] suggested the relative standard deviation of the inverse of the measured interfacial velocity to characterize the relative bubble velocity fluctuation with the following form

$$\frac{V'_b}{\overline{V}_b} \approx \frac{1}{0.85} \cdot \frac{\sqrt{\overline{\left(1/\vec{v}_{szj} - \overline{(1/\vec{v}_{szj})}\right)^2}}}{\overline{(1/\vec{v}_{szj})}}. \tag{8}$$

where 0.85 was determined by their numerical analysis. When the bubble diameters were in the range from $1.2\Delta s$ to $3\Delta s$, the authors reported the error of the above relation was in ±10%, where Δs denoted the distance between the two tips of the double-sensor probe.

3. Experimental facility and instrumentation

3.1. Experimental loop and test sections

The experimental loop is schematically illustrated in Fig. 1. The test section was a round transparent tube made of acrylic resin. Its inner diameter and length were 40 and 2000 mm, respectively. The working fluids in operation were air and water. The water was circulated in the loop by a centrifugal pump. The air, supplied by a compressor, was introduced into the test section through a mixing chamber. Both the flow rates of air and water were measured by rotameters. Fig. 2 shows the schematic diagram of the mixing chamber. The bubbles, with the diameters ranged from 1 to 3 mm, were generated by 25 pieces of glasscapillarys located in the mixing chamber. The inner diameter of the glasscapillary was 0.5 mm. The interfacial area concentration, void fraction and bubble Sauter mean diameter were measured using both digital high-speed camera system and a double-sensor conductivity probe. The measurements by digital high-speed camera system were performed at the axial location of 1700 mm from the bottom of the test section, where a light compensation box was built to eliminate ill effects of refraction and reflection caused by the round pipe. The local flow measurements using a double-sensor conductivity probe were carried out at the axial location of 1780 mm.

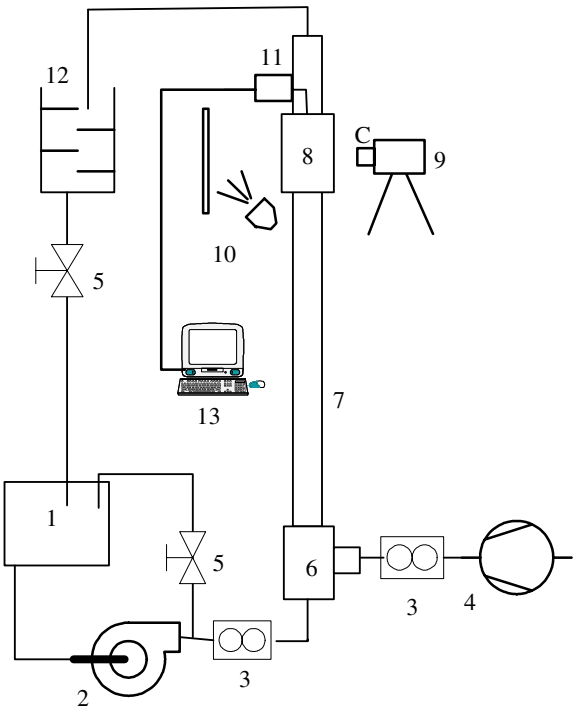

Fig. 1. Schematic diagram of experimental loop. 1—water tank, 2—water pump, 3—flow meter, 4—compressor, 5—flow control valve, 6—mixing chamber, 7—test section, 8—light compensation box, 9—digital high-speed camera system, 10—light source, 11—double-sensor conductivity probe system, 12—phase seperator, 13—PC.

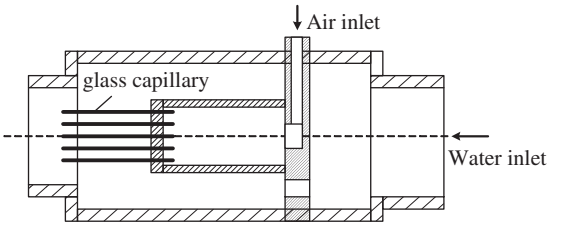

Fig. 2. Schematic diagram of the mixing chamber.

3.2. Double-sensor conductivity probe methodology

The double-sensor probe measurement and benchmark system is schematically shown in Fig. 3. The measurement system consisted of a double-sensor conductivity probe, a mechanical traverser, a measurement circuit, a digital high-speed acquisition board, and the software used to signal processing. The double-sensor conductivity probe was attached to the mechanical traverser mounted on a specially designed flange, and it could be moved back and forth along the radial direction of the test section. The measurement circuit was used to measure the potential difference between the exposed tip and the grounded terminal. A high-speed NI PCI-6110E acquisition board and a personal computer was used to acquire the voltage signal of the double-sensor probe, with the help of a control program developed under NI LabView software environment. The sampling frequency was set 30 kHz for each sensor, and the sampling time was 40 s.

Fig. 4 shows the schematic diagram of the double-sensor conductivity probe. The probe sensors were made of stainless steel wire with a diameter of 0.15 mm. To build the probe, each wire was acuminated through chemical corrosion method, and then insulated with insulating varnish keeping the tip exposed about 0.2 mm. Both wires were inserted into a 0.9 mm inner diameter stainless steel tube with 90° elbow. The two wires were adjusted for the tips separation of about 2 mm, and were bounded to the stainless steel tube with high strength epoxy cement. As for the double-sensor conductivity probe used in this paper, the distance between the two tips was 1.84 mm.

When the probe sensor is surrounded by liquid, a lower voltage is put out; and when the probe sensor contacts with gas, a higher voltage is obtained. But due to the finite size of each sensor and the time delay needed to wet or rewet the sensor tips, the output signal of the double-sensor probe differed from ideal two-state square-wave. A suitable signal processing technique is therefore necessary to extract the required information from the raw signal. In the present work, a method suggested by Angeli and Hewitt [23] was used to regenerate the ideal square-wave signal. Signals before and after processing using this method are illustrated in Fig. 5.

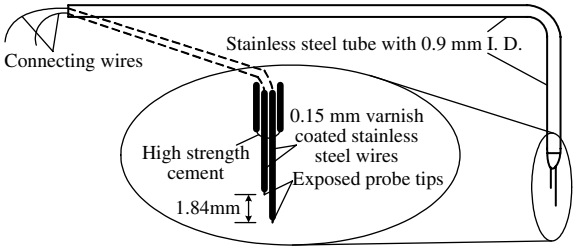

Fig. 4. Schematic diagram of the double-sensor conductivity probe.

From the ideal square-wave signal shown in Fig. 5, the number of bubbles that hit the sensor, N_t, can be measured by counting the number of pulses in the signal. The interfacial velocity in the main flow direction of each interface can be obtained by the distance between the two tips of the double-sensor probe, Δs, and time delay between the upstream and downstream signal

$$\vec{v}_{szj} = \frac{\Delta s}{(T_{DR} - T_{UR})_j}. \tag{9}$$

From the local instant formulation of the two-fluid model, the local time-averaged void fraction can be expressed as the ratio between the accumulated pulse widths of the upward or downward sensor and the total sampling time during the sampling period

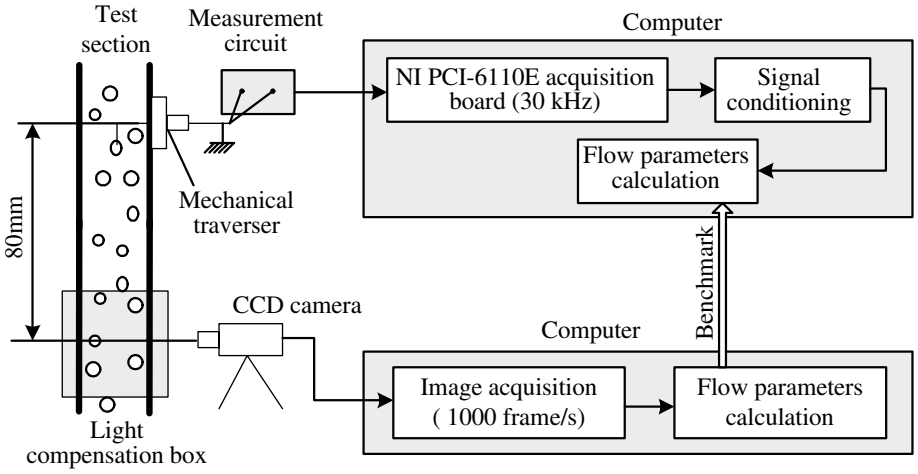

Fig. 3. Schematic of double-sensor conductivity probe measurement and benchmark system.

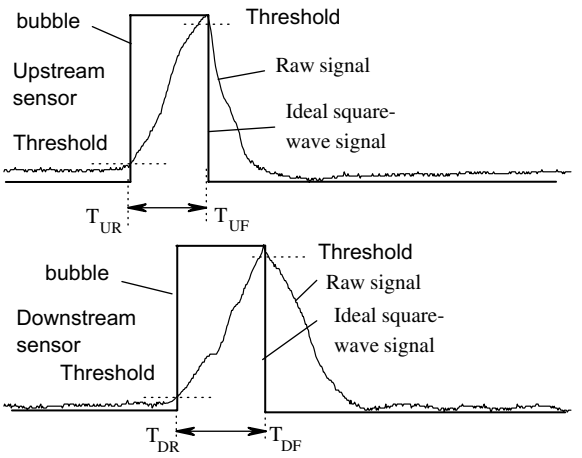

Fig. 5. Illustration of signals before and after the signal processing.

$$\bar{\alpha}^t = \frac{1}{\Delta T}\sum_{j}^{N_s}(T_{UF} - T_{UR})_j. \tag{10}$$

The local time-averaged interfacial area concentration can be obtained through statistical analysis of the measured interfacial velocity or the length of pulse of each bubble using the mentioned statistical model in Section 2.

3.3. Digital high-speed camera system methodology

A SpeedCam Pro-LT digital high-speed camera system, which could run up to 5000 frame/s, was used to visualize the bubbly flow. In the present work, the sampling frequency was set to 1000 frame/s. Typical photographic image for bubbly flow from digital high-speed camera system is illustrated in Fig. 6.

In order to get the interfacial area and volume of each bubble from the photographic image, the bubbles were assumed to be an ellipsoid of revolution rotated around the minor axis. The MsPaint software for image processing was used to determine the minor and major axis lengths, a and b, for each bubble. Then according to Hibiki et al. [5], the interfacial area A and the volume V of a bubble with that shape were calculated by

$$A = 2\pi\left(b^2 + \frac{ba^2}{2\sqrt{b^2-a^2}}\ln\frac{b+\sqrt{b^2-a^2}}{b-\sqrt{b^2-a^2}}\right), \tag{11}$$

$$V = \frac{\pi}{6}ab^2. \tag{12}$$

Based on the results of statistical analysis of interfacial areas and volumes of all bubble in the given flow region, we could obtain the averaged interfacial area concentration and void fraction. In order to remove stochastic error, three photographic images of different time were processed for the same flow condition. The resolution of the photographic image was 512×512 pixel, corresponding to ± 0.1 mm precision in the measurement of the bubble minor and major axis lengths. As for the measurement of interfacial area concentration and void fraction, the errors were 9.3% and 13.4%, respectively.

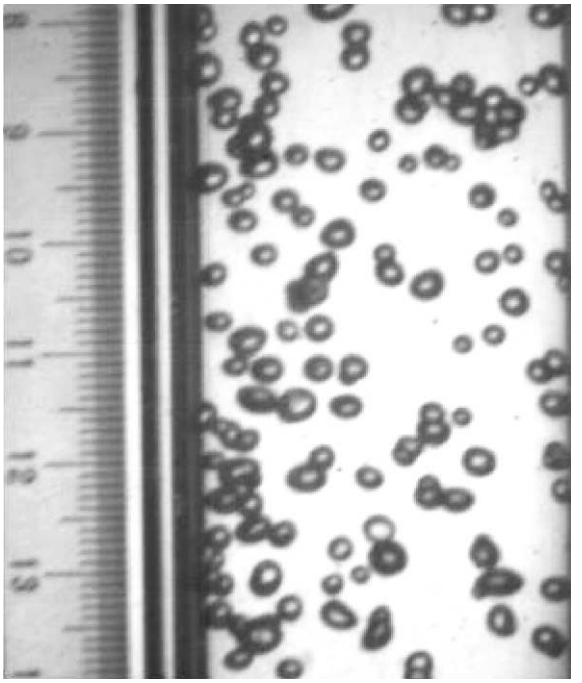

Fig. 6. Typical photographic image from digital high-speed camera.

4. Results and discussion

4.1. Comparison of models for local interfacial area concentration measurement

Fig. 7 display the comparison of local interfacial area concentration profiles calculated using the statistical models derived by Kataoka et al., Kalkach-Navarro et al., Hibiki et al., and Wu and Ishii. The liquid superficial velocity is $J_W = 0.442$ m/s, and the gas superficial velocities include: (a) $J_G = 0.011$ m/s, (b) $J_G = 0.044$ m/s, and (c) $J_G = 0.090$ m/s. Here r/R is the ratio between the probe radial location from the pipe center, r, and the pipe radius, R. From the figures we can see that each of the four statistical models can give the typical "saddle" pattern distribution of local interfacial area concentration in three different flow conditions, with obvious peaks near the wall of the pipe. However, the values of local interfacial area concentration obtained by different statistical models differ a lot from each other. Generally, in the same flow condition and at the same measurement

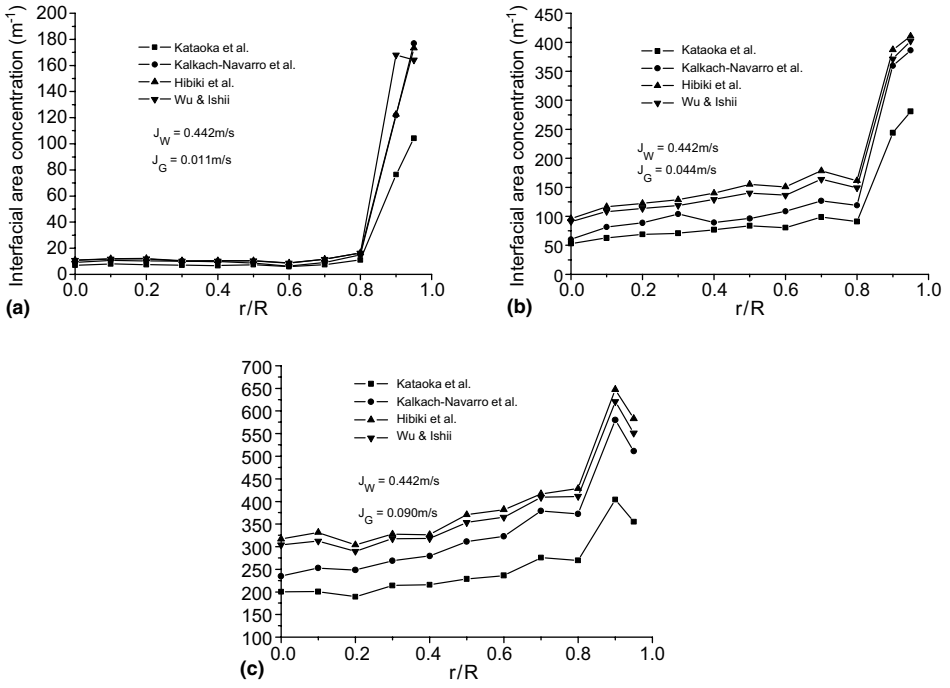

Fig. 7. Interfacial area concentration profiles calculated by statistical models of different researchers based on the same signals of double-sensor conductivity probe: (a) $J_G = 0.011$ m/s, (b) $J_G = 0.044$ m/s, and (c) $J_G = 0.090$ m/s.

location, the local interfacial area concentrations increase in the order of Kataoka et al., Kalkach-Navarro et al., Wu and Ishii, and Hibiki et al. Especially when gas superficial velocity is larger (for example, J_G = 0.044 m/s and J_G = 0.090 m/s), the discrepancies among the local interfacial area concentration profiles calculated using different statistical models become more visible. This suggests that, when using a double-sensor probe to measure the local interfacial area concentration in bubbly flow, we must make a right choice for the statistical models.

4.2. Verification for double-sensor probe methodology

In order to evaluate the accuracy and reliability of the different statistical models, the interfacial area concentration measured by a double-sensor conductivity probe is compared with experimental data of digital high-speed camera system. The liquid superficial velocity is 0.442 m/s, and the gas superficial velocities are ranged from 0.011 to 0.033 m/s. Using digital high-speed camera system, however, only volume-averaged interfacial area concentration, void fraction, and bubble Sauter mean diameter can be obtained. Assuming that the axial change of the flow parameters between the locations of double-sensor probe and high-speed camera can be neglected, the section-averaged flow parameters measured by a double-sensor conductivity probe should be equal to the volume-averaged values by the digital high-speed camera system. The section-averaged flow parameters measured by a double-sensor conductivity probe are given by $\langle \phi \rangle_A \equiv \frac{1}{A}\int_0^R 2\pi r \phi(r)\,\mathrm{d}r$, where A is the cross-sectional area of the test section.

As shown in Fig. 8(a), with increasing gas superficial velocity, the averaged void fraction measured by digital high-speed camera system and by double-sensor conductivity probe can agree well. Comparisons of the averaged interfacial area concentration by different statistical models for local interfacial area concentration measurement against data of digital high-speed camera system are illustrated in Fig. 8(b). We can see that the statistical model by Kataoka et al. gives the best agreement with experimental data of digital high-speed camera system, within the relative deviation of 12.7%. The statistical models derived by Kalkach-Navarro et al., Wu and Ishii, and Hibiki et al. overestimate with relative deviations of 45.7%, 69.3%, and 63.2%, respectively. According to Hibiki et al. [5], the local bubble Sauter mean diameter, d_{sm}, can be expressed as $d_{sm} = 6\alpha/a_i$. Fig. 8(c) displays the comparisons of averaged bubble Sauter mean diameter calculated by interfacial area concentration against experimental data of digital high-speed camera system. As shown in the figure, using statistical models of Kalkach-Navarro et al., Wu and Ishii, and Hibiki et al., the averaged bubble Sauter mean diameters

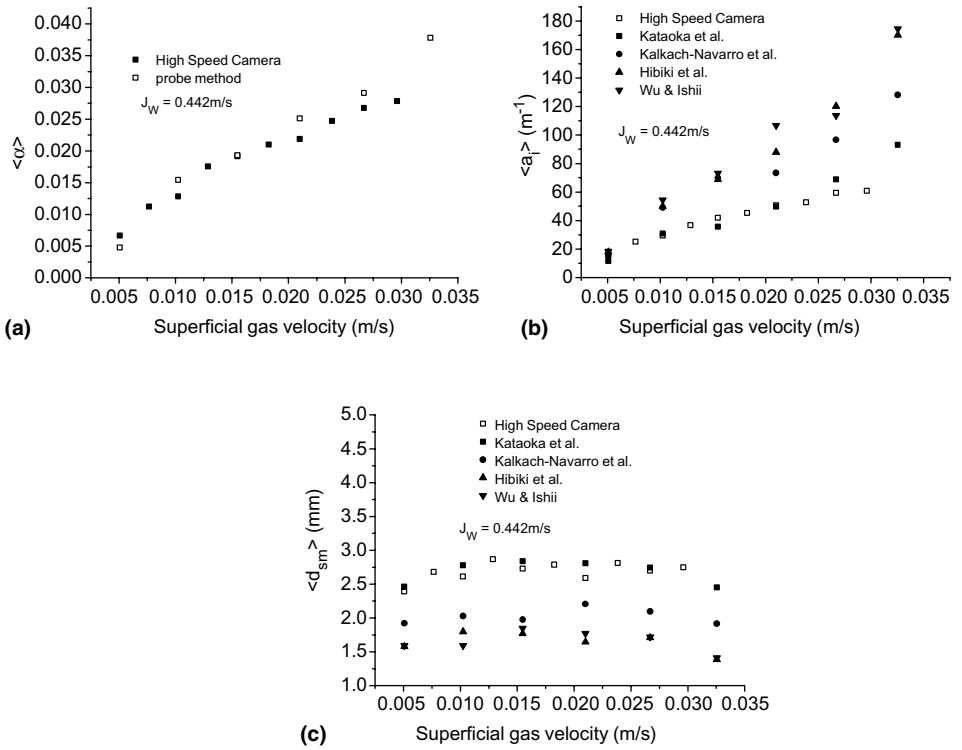

Fig. 8. Comparisons of average flow parameters measured by double-sensor conductivity probe against digital high-speed camera system: (a) void fraction, (b) interfacial area concentration, and (c) bubble Sauter mean diameter.

are underestimated with relative deviations of 21.4%, 36.7%, and 34.5%, respectively. The values of bubble Sauter mean diameters by Kataoka et al.'s statistical model are coincident with experimental data of digital high-speed camera system within relative deviations of 5.7%. This implies that the statistical model of Kataoka et al. is more reasonable than the other three ones. Therefore, when carrying out experiments to measure the local interfacial area concentration in bubbly flow using a double-sensor conductivity probe, the statistical model of Kataoka et al. is recommended in this paper.

4.3. Local flow parameters

Using the verified double-sensor probe method, we carry out experiment to study the local distribution characteristic of the interfacial area concentration and void fraction in fully-developed bubbly flow in a round

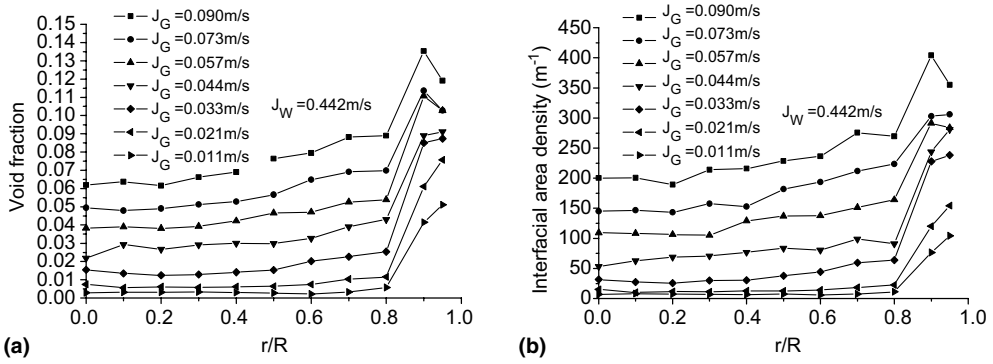

Fig. 9. Local flow parameters profiles measured by double-sensor conductivity probe: (a) local void fraction, (b) local interfacial area concentration obtained by Kataoka et al.'s [3] statistical model.

pipe. The liquid superficial velocity is 0.442 m/s, and the gas superficial velocities are ranged from 0.011 to 0.09 m/s. For all flow conditions, the bubbly flow regime was observed. In Fig. 9(a), the radial profiles of the void fraction measured by double-sensor conductivity probe are shown. It can be seen that the local void fraction displays typical "saddle" pattern distribution with an obvious peak near the wall of the pipe at about $r/R \approx 0.85$. This is because the composition of lift force, wall lubrication force and turbulent dispersion force provokes the migration of bubbles toward pipe wall. With an increase of gas superficial velocity, the local void fraction increases for all flow conditions, and the locations of the wall peak of local void fraction move slightly against the pipe wall. The radial profiles of the local interfacial area concentration obtained using the statistical model suggested by Kataoka et al. show a very similar behavior to the void fraction profiles, as illustrated in Fig. 9(b). The local interfacial area concentration also has a peak near the wall of the pipe, and is flat at the center for nearly all gas flow. The wall peak of local interfacial area concentration can go up to 400 m^{-1} at about $r/R \approx 0.90$. With increasing gas superficial velocity, the local interfacial area concentration rises over a cross-section of the flow channel.

5. Conclusions

Based on the experimental data of digital high-speed camera system, four statistical models for local interfacial area concentration measurement using double-sensor conductivity probe were evaluated. All the four statistical models can give the typical "saddle" pattern distribution of local interfacial area concentration with obvious peaks near the wall of the pipe. However, there are great differences in the values of local interfacial area concentration obtained by different statistical models even from the same probe signals.

With increasing gas superficial velocity, the averaged void fractions measured by digital high-speed camera system and by double-sensor conductivity probe can agree well. The interfacial area concentration obtained by the statistical model by Kataoka et al. gives the best agreement with results of digital high-speed camera system. The statistical models derived by Kalkach-Navarro et al., Wu and Ishii, and Hibiki et al. overestimate as a whole. Therefore, when carrying out experimental investigation of the local interfacial area concentration in bubbly flow using a double-sensor conductivity probe, the statistical model of Kataoka et al. is recommended. Using the verified double-sensor probe method, we carry out experiment to study the local distribution characteristic of the interfacial area concentration and void fraction in air–water bubbly flow through a vertical pipe.

Acknowledgement

We gratefully acknowledge the National Science Foundation of China (contract no. 10172069) and National Basic Research Program of China (contract no. 2003CB214500).

References

[1] L.J. Guo, Two-phase and Multiphase Flow Dynamics, Xi'an Jiaotong University Press, Xi'an, 2002, pp. 155–179.
[2] M. Ishii, Thermo-fluid dynamic theory of two-phase flow, Eyerolles, France, Paris, 1975.
[3] I. Kataoka, M. Ishii, A. Serizawa, Local formulation and measurement of interfacial area concentration in two-phase flow, Int. J. Multiphase Flow 12 (4) (1986) 505–529.
[4] S. Kalkach-Navarro, R.T. Lahey Jr., D.A. Drew, R. Meyder, Interfacial area density, mean radius and number density measurements in bubbly two-phase flow, Nucl. Eng. Des. 142 (1993) 341–351.
[5] T. Hibiki, H. Hogsett, M. Ishii, Local measurement of interfacial area, interfacial velocity and liquid turbulence in two-phase flow, Nucl. Eng. Des. 184 (1998) 287–304.
[6] K.X. Sun, M.Y. Zhang, X.J. Chen, Interfacial area concentration in horizontal two-phase bubbly flow, J. Xi'an JiaoTong University 33 (6) (1999) 24–28.
[7] K.X. Sun, M.Y. Zhang, X.J. Chen, Experimental study of local statistical parameters in horizontal gas–liquid two-phase bubbly flow, Chin. J. Nucl. Sci. Eng. 19 (3) (1999) 228–234.
[8] G. Kocamustafaogullari, W.D. Huang, J. Razi, Measurement and modeling of averaged void fraction, bubble size and interfacial area, Nucl. Eng. Des. 148 (1994) 437–453.
[9] T. Hibiki, Y. Mi, R. Situ, M. Ishii, Interfacial area transport of vertical upward bubbly two-phase flow in an annulus, Int. J. Heat Mass Transfer 46 (2003) 4949–4962.
[10] X.D. Sun, S. Kim, L. Cheng, M. Ishii, S.G. Beus, Interfacial structures in confined cap-turbulent and churn-turbulent flows, Int. J. Heat Fluid Flow 25 (2004) 44–57.
[11] S. Kim, M. Ishii, Q. Wu, D. McMreary, S.G. Beus, Interfacial structures of confined air–water two-phase bubbly flow, Exp. Thermal Fluid Sci. 26 (2002) 461–472.
[12] O. Zeitoun, M. Shoukri, V. Chatoorgoon, Measurement of interfacial area concentration in subcooled liquid–vapour flow, Nucl. Eng. Des. 152 (1994) 143–255.
[13] Q. Wu, M. Ishii, Sensitivity study on double-sensor conductivity probe for the measurement of interfacial area concentration in bubbly flow, Int. J. Multiphase Flow 25 (1) (1999) 155–173.
[14] I. Kataoka, M. Ishii, A. Serizawa, Sensitivity analysis of bubble size and probe geometry on the measurements of interfacial area concentration in gas–liquid two-phase flow, Nucl. Eng. Des. 146 (1994) 53–70.
[15] K. Sekoguchi, H. Fukui, T. Matusoka, K. Nishikawa, Studies on statistical characteristics of bubbles by electrical resistivity probe, I, II, Trans. JSME 40 (1974) 2295–2310.

[16] S.G. Dias, F.A. Franca, E.S. Rosa, Statistical method to calculate local interfacial variables in two-phase bubbly flows using intrusive crossing probes, Int. J. Multiphase Flow 26 (2000) 1797–1830.
[17] T. Wilmarth, M. Ishii, Interfacial area concentration and void fraction of two-phase flow in narrow rectangular vertical channels, ASME Trans. J. Fluids Eng. 119 (1997) 916–922.
[18] J.M. Delhaye, P. Bricard, Interfacial area in bubbly flow: experimental data and correlation, Nucl. Eng. Des. 151 (1994) 65–77.
[19] T. Tomida, F. Yusa, T. Akazaki, Effective interfacial area and liquid-side mass transfer coefficient in the upward two-phase flow of gas–liquid mixtures, Chem. Eng. J. 16 (2) (1978) 81–88.
[20] B.A.A. Woezik, K.R. Westerterp, Measurement of interfacial areas with the chemical method for a system with alternating dispersed phase, Chem. Eng. Process. 39 (2000) 299–314.
[21] E.J. Molga, K.R. Westerterp, Experimental study of a cocurrent upflow packet bed bubble column reactor: pressure drop, holdup and interfacial area, Chem. Eng. Process. 36 (1997) 489–495.
[22] S.L. Kiambi, A.M. Duquenne, A. Bascoul, H. Delmas, Measurements of local interfacial area: application of bi-optical fibre technique, Chem. Eng. Sci. 56 (2001) 6447–6453.
[23] P. Angeli, G.F. Hewitt, Flow structure in horizontal oil–water flow, Int. J. Multiphase Flow 26 (2000) 1117–1140.